Promotional effect of metal encapsulation on reactivity of iron oxide supported Pt catalysts

Y.-N. Sun, M. Lewandowski, Z.-H. Qin[1], S. Shaikhutdinov*, H.-J. Freund

Abteilung Chemische Physik, Fritz-Haber-Institut der Max-Plank-Gesellschaft, Faradayweg 4-6, 14195 Berlin, Germany

Abstract: We studied reactivity of well-defined Pt model catalysts, supported on crystalline iron oxide Fe_3O_4(111) films, in low temperature CO oxidation. It is shown that pre-annealing in vacuum at ~850 K suppresses CO adsorption but increases CO_2 production rate. This finding is rationalised in terms of Strong Metal-Support Interaction between Pt and iron oxide resulting in particles encapsulation by a thin FeO(111) film that catalyses CO oxidation similarly to the extended FeO(111)/Pt(111) surfaces previously studied (*Sun et al. J. Catal, 266 (2009) 359*). The results show that the stability and the atomic structure of the encapsulated layer under reaction conditions play a critical role in oxidation reactions over Pt catalysts supported on reducible oxides.

Keywords: platinum, iron oxides, strong metal-support interaction, CO oxidation

* Correpsonding author: E-mail shaikhutdinov@fhi-berlin.mpg.de

[1] Present address: Wuhan Institute of Physics and Mathematics, Chinese Academy of Sciences, 430071 Wuhan, P. R. China

1. Introduction

Strong Metal-Support Interaction (SMSI) is generally defined as a close chemical and physical interaction between the metal and support. SMSI was originally developed as an explanation for the decreased chemisorption of CO and H_2 on metal particles, and was most notably observed for Pt supported on TiO_2 upon high temperature reduction [1,2]. A well-documented physical manifestation of SMSI is the encapsulation of metal particles by the reduced oxide support [3-6], which is believed to be a result of minimization of surface energy of systems consisting of metals having relatively high surface energy (such as Pt, Pd) and oxides with relatively low surface energy (e.g, titania, ceria) [7]. Obviously the encapsulation suppresses catalytic reactions on metal surfaces. However, reaction conditions may alter the surface structure of the encapsulated overlayer and hence the reactivity of a catalyst. In addition, the limited thickness of the oxide films often only a few Angstroms in size may control electron transfer to surface bound species rendering them active (see [8] and references therein). Very recently it was experimentally observed that thin oxide films on metals, indeed, may exhibit enhanced catalytic activity [9,10]. The example studied was CO oxidation on an ultra-thin FeO(111) film grown on a Pt(111) single crystal. It was suggested that under reaction conditions the bi-layer FeO film transforms into the tri-layer O-Fe-O film that catalyses CO oxidation in the mbar pressure range at relatively low temperatures, ~ 450 K [10]. Further studies including density functional theory calculations corroborated this scenario [11].

In order to see whether the promotional effect of thin oxide films on reactivity is present for highly dispersed metal catalysts, we studied here CO oxidation on Pt particles supported on Fe_3O_4(111) films. It has previously been shown that the Pt particles can be encapsulated by an iron oxide film which is structurally very similar to FeO(111) on Pt(111) [6]. This allows us to perform a comparative study of reactivity of clean and encapsulated Pt particles in light of results observed on single crystal surfaces.

2. Experimental

The experiments were performed in two UHV chambers ("TPD-GC" and "STM") equipped with low energy electron diffraction (LEED), Auger electron spectroscopy (AES) and a quadrupole mass spectrometer (QMS) for temperature programmed desorption (TPD) studies. The TPD-GC chamber houses a "high-pressure" reactor (~ 30 ml, made of Au-plated massive Cu block) connected to a gas chromatograph GC 6890N (Agilent). The double-side polished Pt(111) crystal (10 mm in diameter, 1.5 mm in thickness) is spot-welded to two parallel Ta wires which are in turn welded to two Ta sticks used for resistive heating and also for cooling by filling a manipulator rod with liquid nitrogen. The temperature is measured by a chromel-alumel thermocouple spot-welded to the edge of the crystal. The manipulator rod inside the chamber ends with a KF-type flange with a 4 pin electrical feedthrough holding Ta and thermocouple sticks. The reactor is sealed with a Viton O-ring placed on top of the reactor matching the flange on the rod.

In the STM chamber, the Pt(111) crystal is mounted to a Pt sample holder. The temperature is controlled using a chromel-alumel thermocouple spot-welded to the edge of the crystal. The crystal can be heated in the UHV chamber by electron bombardment from the backside using a tungsten filament. For treatments at high pressures the sample is transferred into the gold-plated reactor (~ 1 l) housing a heating stage whereby the sample is heated radiatively from the backside using a halogen lamp.

The ~ 10 nm thick Fe_3O_4(111) films were grown by repeated cycles of Fe deposition at 300 K and oxidation in 10^{-6} mbar O_2 at ~ 900 K for 5 min with the final oxidation step at ~ 1000 K for 10 min. Iron and Pt (both 99.95%, from Goodfellow) were deposited using e-beam assisted evaporators (Focus EFM3, Omicron). During deposition, the sample was biased with a retarding potential to prevent metal ions from being accelerated towards the sample. Prior to Pt deposition, the Fe_3O_4(111) films were flashed to ~900 K in UHV to form a single termination oxide surface as judged by STM. It should be noticed that the Pt coverage (in monolayers (ML), 1 ML corresponds to 1.5 x 10^{15} at/cm^2) was measured by STM for structural studies, while a quartz microbalance was employed for samples used in reactivity studies. This may cause deviation in the absolute numbers for Pt coverages in two experimental setups.

CO (99.995%, Linde) and O_2 (99.999%, AGA GmbH) were additionally cleaned using a cold trap at ~ 150 K. For reactivity measurements the reaction mixture of CO and O_2

was balanced by He to 1 bar. The gas was circulating through the reactor with a flow of ~3 ml/min and analyzed by GC (HP-Plot Q column at 35°, TCD detector).

3. Results and discussion.

Nucleation and growth of Pt particles on Fe_3O_4(111) films have previously been studied in our laboratories by STM and TPD [6,12,13]. Figure 1 shows typical large-scale STM images of Pt deposited onto the film at room temperature and subsequently annealed in UHV at 600 K (a,c) and 850 K (b,d). Obviously high-temperature annealing causes sintering and faceting of the Pt particles. At sub-monolayer coverages Pt additionally forms islands of two Pt(111) layers in thickness as shown in the inset in Fig. 1b (see also [12]). At high Pt coverage, the particles expose atomically flat top facets which are Pt(111) in nature due to the good epitaxial relationships between Fe_3O_4(111) and Pt(111) [6].

Annealing at 850 K is accompanied by strong reduction of the CO uptake (at least, by factor of 3 as compared to the samples annealed to 600 K) which drops almost to zero in the case of high Pt coverages as measured by TPD (not shown here). This is a "classical" manifestation of SMSI and has previously been rationalised in terms of particle encapsulation by a FeO-like ultra-thin film [6,12]. In this study, atomically resolved STM images provide compelling evidence. Figure 1f and, more clearly, the inset in Fig. 1d show that the top facets of the largest Pt particles exhibit the hexagonal lattice of protrusions with a ~3 Å periodicity, in turn forming the superstructure with a ~25 Å periodicity. This structure is well documented in the literature for iron oxide films grown on Pt(111) [14,15] and can unambiguously be assigned to a monolayer FeO(111) film which consists of close-packed layers of iron and oxygen stacked as O-Fe-Pt(111), as schematically shown in Fig. 1e. The Moire superstructure originates from a ~ 10 % mismatch between the Pt(111) and FeO(111) lattices. Henceforth we will refer to Pt annealed to 850 K as an "encapsulated" system to discriminate from a "clean" Pt/Fe_3O_4 system annealed to 600 K, although in the latter case partial Fe-Pt intermixing is observed as the initial stage of the encapsulation [13].

Model Pt/Fe_3O_4 catalysts were examined with respect to CO oxidation at the stoichiometric ratio (40 mbar CO; 20 mbar O_2, He balance), and under O-rich conditions (10 mbar CO; 50 mbar O_2, He balance). Figure 2 shows kinetic curves of CO_2 production at 450

K on clean (solid symbols) and encapsulated (open symbols) Pt particles at two coverages (1.6 and 6.3 ML). The results for pristine Fe_3O_4(111) films under the same conditions are also shown, for comparison.

It is worth recalling that CO oxidation on Pt proceeds via the Langmuir-Hinshelwood mechanism whereby CO_2 is formed through the associative reaction of chemisorbed CO with the oxygen surface atoms produced by dissociation of molecular oxygen [16]. The reaction has two distinct branches in the activity vs CO/O_2 ratio dependence, reflecting the competition for adsorption sites between O_2 and CO. Oxidation of CO on iron oxides likely proceeds through the Mars-van Krevelen scheme, typically considered for reducible oxides, whereby CO removes the lattice oxygen which is then replenished by reaction with molecular O_2 [17,18].

Figure 2 shows that the activity of Pt/Fe_3O_4 catalysts increases with increasing Pt coverage. In addition, the average reaction rate increases by a factor of ~2, upon increasing oxygen pressure from 20 to 50 mbar, in fair agreement with the reaction order for O_2 (n ~ 0.85) measured on a Pt(111) single crystal under the same experimental conditions [10]. The results suggest that CO oxidation primarily occurs on Pt particles rather than on Pt/support interface. In the latter case, the reactivity would have been higher at low Pt coverage apparently having the higher number of interfacial cites as shown by STM (see Fig. 1). Note, however, that in an O-rich ambient, the reactivity of the Fe_3O_4(111) support is greatly enhanced and becomes comparable with the Pt particles formed at low coverage. This finding suggests a positive reaction order for O_2, that is at variance with the zero-order observed on powdered Fe_2O_3 catalysts, although at much higher temperatures (520 – 570 K) than used here (450 K) [19,20]. The discrepancy may also be related to the different red-ox properties of magnetite (Fe_3O_4) and hematite (Fe_2O_3) surfaces.

However, the most intriguing result revealed in these experiments is the higher reactivity of the encapsulated Pt particles as compared to their clean counterparts. This effect is clearly observed for the high Pt coverage at both $CO:O_2$ ratios studied. At low Pt coverage, the catalysts showed comparable activities despite the encapsulated system exposed much less Pt surface atoms, by factor of 2-3 as compared to the clean system, as measured by the CO uptake. This finding suggests that, at low Pt coverage, the encapsulated Pt surface is, at least, as active as the clean Pt.

The rate enhancement can tentatively be linked to the presence of the FeO(111) film covering Pt particles which has previously been shown to greatly promote CO oxidation when grown on a Pt(111) single crystal [10]. The proposed mechanism [10,11] includes structural transformations of the FeO bi-layer into the OFeO tri-layer film under oxygen partial pressures in the mbar range (see the scheme in Fig. 3). To see whether this restructuring occurs also on dispersed Pt, we have performed STM study of encapsulated Pt particles exposed to 20 mbar of O_2 at 450 K. Figure 3 shows that the large-scale morphology is not much altered by this treatment: The average size and height of the particles remain essentially the same. However, the superstructure seen on top of the O_2-treated particles (see Fig. 3b) exhibits the hemispherical shape of large protrusions with a ~1.0 Å corrugation amplitude (see profile line in Fig. 3c), whereas the pristine FeO layer shows a honeycomb-like structure with a smaller corrugation amplitude (~0.5 Å, on average, see Fig. 1f) at similar tunneling conditions. Essentially the same picture has been observed by STM for a FeO(111) film on a Pt(111) crystal upon oxidation [11]. This similarity suggests that the surface of the encapsulated Pt particles restructures in oxygen in the same manner as the extended FeO(111)/Pt(111) surface, ultimately resulting in higher reactivity than of clean Pt particles.

Figure 2 also shows that the reaction slows down in time, particularly at low oxygen pressure. The catalysts deactivation seems to be assigned to carbon deposition as observed on the spent catalysts by AES. Carbon is most likely formed by CO dissociation on open Pt sites either present to some extent on the small Pt particles from the beginning as judged by CO TPD, or developed in the course of the film dewetting [9,10]. In principle, carbon deposition may partially reduce the iron oxide film thus attenuating the promotional effect of the encapsulation. Since CO dissociation primarily occurs on low-coordinated sites [13,21], the overall effect may be size-dependent.

4. Conclusions

This comparative study of Pt model catalysts supported on Fe_3O_4(111) films in low temperature CO oxidation shows rate enhancement upon high temperature annealing in vacuum. This finding is attributed to the encapsulation of the Pt particles by a thin FeO(111) film as directly shown by high-resolution STM. The FeO overlayer on Pt promotes CO

oxidation in the same way as has recently been observed on a Pt(111) single crystal. The mechanism includes oxygen induced transformation of the FeO bi-layer film into the tri-layer O-Fe-O film that catalyses CO oxidation. The results indicate that the stability and the atomic structure of the encapsulated layer under reaction conditions play a critical role in oxidation reactions on Pt catalysts supported on reducible oxides.

Acknowledgements.

We acknowledge support from DFG through the Cluster of Excellence "Unifying concepts in catalysis" (UNICAT), coordinated by TU Berlin, and the Fonds der Chemischen Industrie.

References

[1] S. J. Tauster, Acc. Chem. Ress., 20 (1987), 389-394.

[2] G. L. Haller, D. E. Resasco, Adv. Catal., 36 (1989), 173-235.

[3] O. Dulub, W. Hebenstreit, U. Diebold, Phys. Rev. Lett., 84 (2000), 3646-3649.

[4] M. Bowker, P. Stone, P. Morrall, R. Smith, R. Bennett, N. Perkins, R. Kvon, C. Pang, E. Fourre, M. Hall, J. Catal., 234 (2005), 172-181.

[5] F. Silly, M.R. Castell, J. Phys. Chem. B, 109 (2005), 12316-12319.

[6] Z.H. Qin, M. Lewandowski, Y.N. Sun, S. Shaikhutdinov, H.-J. Freund, J. Phys. Chem. C, 112 (2008), 10209-10213.

[7] H. Knözinger, E. Taglauer, in: G. Ertl; H. Knözinger, J. Weitkamp (Eds.), Handbook of Heterogeneous Catalysis, VCH Weinheim, 1997, pp. 216 – 231.

[8] H.-J. Freund, G. Pacchioni, Chem. Soc. Rev., 37 (2008), 2224-2242.

[9] Y.N. Sun, Z.H. Qin, M. Lewandowski, S. Shaikhutdinov, H.J. Freund, Catal. Letters, 126 (2008), 31-35.

[10] Y.N. Sun, Z.H. Qin, M. Lewandowski, E. Carrasco, M. Sterrer, S. Shaikhutdinov, H.-J. Freund, J. Catal., 266 (2009), 359-368.

[11] M. Lewandowski, L. Giordano, J. Goniakowski, et al. Angew. Chem. Intern. Ed., submitted.

[12] Z.H. Qin, M. Lewandowski, Y.N. Sun, S. Shaikhutdinov, H.-J. Freund,J. Phys.: Condens. Matter, 21 (2009), 134019 -134025.

[13] Y.N. Sun, Z.H. Qin, M. Lewandowski, S. Shaikhutdinov, H.-J. Freund, Surf. Sci., 603 (2009), 3099-3103.

[14] M. Ritter, W. Ranke, W. Weiss, Phys. Rev. B, 57 (1998), 7240-7251.

[15] H.C. Galloway, P. Sautet, M. Salmeron, Phys. Rev. B, 54 (1996), R11145-R11148.

[16] R. Imbihl, G. Ertl, Chem. Rev., 95 (1995), 697-733.

[17] P. Mars, D.W. van Krevelen, Chem. Eng. Sci., 3 (1954), 41-59.

[18] M.A. Vannice, Catal. Today, 123 (2007), 18-22.

[19] P. Li, D.E. Miser, S. Rabiei, R.T. Yadav, M.R. Hajaligol, Appl. Catal. B, 43 (2003), 151-162.

[20] S. Wagloehner, D. Reichert, D. Leon-Sorzano, P. Balle, B. Geiger, S. Kureti, J. Catal., 260 (2008), 305-314.

[21] K. McCrea, J. Parker, P. Chen, G. Somorjai, Surf. Sci., 494 (2001), 238-250.

Figure captions.

Figure 1. STM images (size 100 nm x 100 nm) of Pt particles supported on Fe_3O_4(111) films annealed in vacuum at 600 (a,c) and 850 K (b,d). Pt coverage is 0.8 ML (a,b) and 2.3 ML (c,d). The insets in (d) and (f) show atomically resolved images of the Pt top facets (presented in (d) in the current mode to increase the contrast). (e) Schematic of Pt particles encapsulated by a FeO(111) layer, and cross section of a FeO(111) film grown on Pt(111). (f) Profile line measured on the Pt top facet. Tunneling parameters are (a) bias 1.4 V, current 1.0 nA; (b-d) 1.4 V, 0.7 nA; insets in (d) and (e) 0.5 V, 0.7 nA.

Figure 2. CO_2 production as a function of time measured on Pt/Fe_3O_4(111) at two Pt coverages and CO and O_2 partial pressures as indicated (He balance). The catalysts were annealed at 600 K (solid symbols) and 850 K (open symbols) prior to reaction. The results for pristine Fe_3O_4(111) films under the same conditions are shown for comparison. Time zero corresponds to the start of heating of a catalyst to the reaction temperature (450 K) with a rate 1 K/sec.

Figure 3. (a) 100 nm x 100 nm STM image of the 2.3 ML Pt/Fe_3O_4(111) surface pre-annealed to 850 K in UHV and then exposed to 20 mbar O_2 at 450 K for 10 min. (b) Zoom in of the Pt particle marked by circle in (a). The profile line along A-B is shown in (c). The scheme shows a proposed O-induced transformation of the bi-layer FeO film into the tri-layer OFeO film. Tunneling parameters are bias 1.4 V, current 0.7 nA.

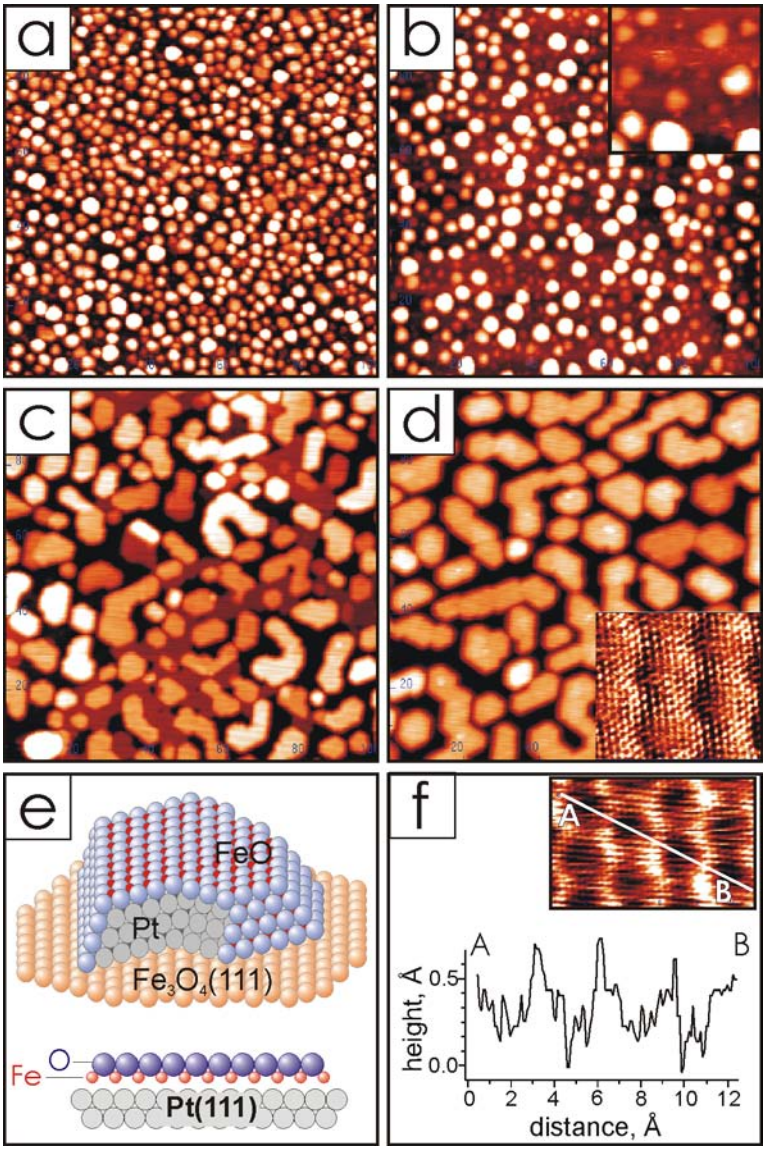
a
b
c
d
e
FeO
Pt
$Fe_3O_4(111)$
Fe
O
Pt(111)
f
A
B
height, Å
0.5
0.0
0
2
4
6
8
10
12
distance, Å

Fig. 1

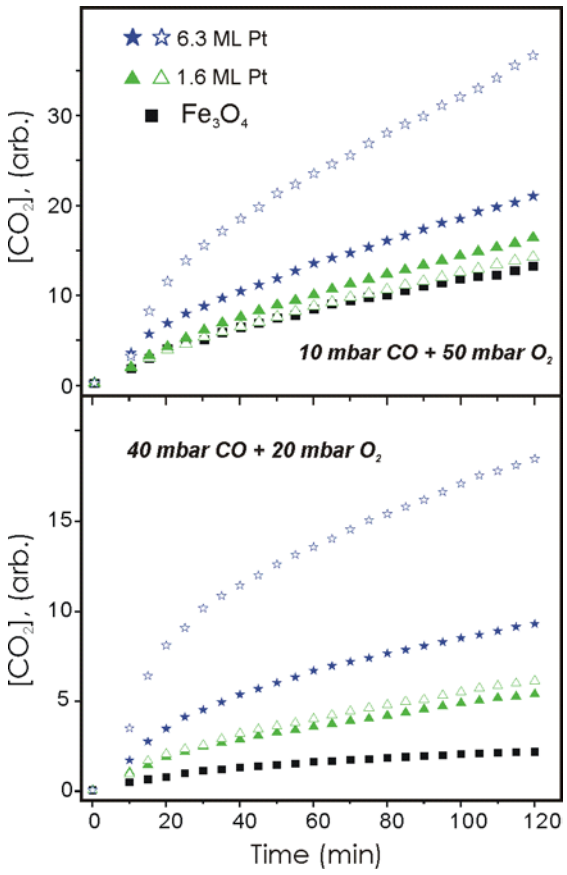
6.3 ML Pt
1.6 ML Pt
Fe3O4
[CO2], (arb.)
10 mbar CO + 50 mbar O2
40 mbar CO + 20 mbar O2
Time (min)

Fig. 2

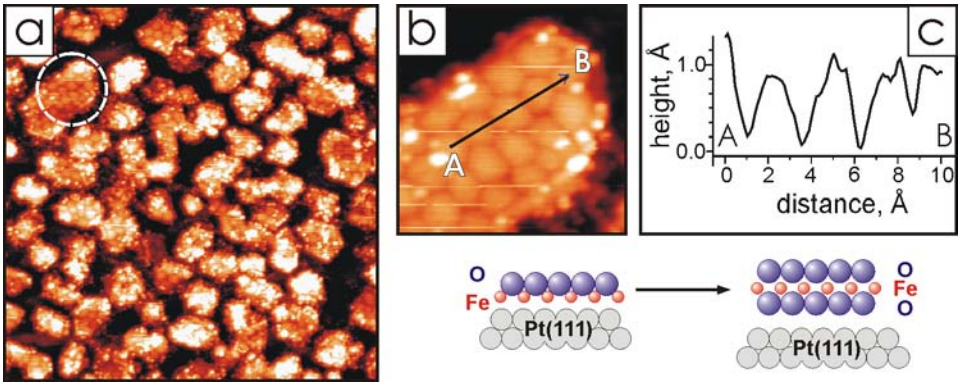
a
b
B
A
c
height, Å
distance, Å
O
Fe
Pt(111)

Fig. 3